PHYSICAL REVIEW B **87**, 100301(R) (2013)

Electric-field effects on the optical vibrations in AB-stacked bilayer graphene

R. Stein, D. Hughes, and Jia-An Yan*

Department of Physics, Astronomy, and Geosciences, Towson University, 8000 York Road, Towson, Maryland 21252, USA

(Received 13 January 2013; revised manuscript received 3 March 2013; published 29 March 2013)

Using first-principles methods, we show that an applied perpendicular electric field E breaks the inversion symmetry of AB-stacked bilayer graphene (BLG), thereby slightly mixing the two in-plane high-energy optical vibrations (E_g and E_u modes). The mixed amplitudes increase parabolically with respect to the field strength when $E < 2.0$ V/nm, and then exhibit linear dependence when $E > 2.0$ V/nm. In contrast, the mixing effect on the out-of-plane vibrations (A_{1g} and A_{2u} modes) is found to be much stronger, with the mixed amplitudes nearly an order of magnitude larger than those for the in-plane modes. For the two in-plane modes, we then calculate their phonon linewidths and frequency shifts as a function of the electric field as well as the Fermi level. Our results reveal delicate interplay between electrons and phonons in BLG, tunable by the applied fields and charge carrier densities.

DOI: 10.1103/PhysRevB.87.100301 PACS number(s): 63.20.kd, 63.22.Rc, 73.22.Pr, 78.30.Na

AB-stacked bilayer graphene (BLG) is a unique platform for which both the charge carrier densities (i.e., the Fermi level E_F) and the band structure can be tuned through applied dual-gate electric fields.[1–3] With an applied external electric field (EEF) of several V/nm, an energy gap opening of up to 250 meV has been reported in gated BLG.[2] Recently, the development of the electrolytic gate has allowed charge carrier densities in BLG doping as high as $|n| \approx 2.4 \times 10^{13}$ cm^{-2}.[4] The tunability on the band structure and the Fermi level reveals rather intriguing properties in this system, including the unusual high-field transport,[5] the renormalization of the phonon energy,[6–8] and the Fano resonance in infrared spectra.[9,10] Interesting device applications such as a hot electron bolometer[11] have also been reported.

Understanding the response of the material's physical properties to external perturbations is crucial for its practical applications. In particular, EEF affects both electronic structure and lattice dynamics, and plays a key role in the performance of electronic devices. Although much attention has been paid to the field effects on the electronic properties of BLG,[2,3,6,12,13] very few studies[14,15] have been conducted on the response of the lattice dynamics to the EEF. Using analytical methods, Ando and Koshino[15] studied the effects of an uneven charge doping and external electric fields on the self-energy of the in-plane modes in BLG. On the other hand, it was proposed more than forty years ago that EEF could be applied to break the symmetry of specific silent modes in $SrTiO_3$ so that it becomes Raman active.[16–18] The electric-field-induced Raman scattering allows study of infrared-active and silent modes in crystals of high symmetry, thus probing the electronic properties of the system. Recent development of tip-enhanced Raman spectroscopy[19] provides a controlled local probe of the response under a nonuniform electric field. However, it is unclear whether such an external perturbation will alter the phonon mode eigenvector itself or not, and to what extent the phonon wave function will be changed, if any.

Raman and infrared (IR) spectroscopy are powerful tools to probe the lattice dynamics of BLG.[6,8,12,13,20–22] A recent IR measurement of gated BLG identified large phonon linewidth ($\sim$30 cm^{-1}) for the mode of frequency $\omega = 1587$ cm^{-1}, which has been ascribed to the in-plane E_u mode,[9] while another IR work[10] ascribed the observed mode to the E_g mode because of broken symmetry. A possible optical mode mixing induced by EEF is also proposed to account for the splitting of the G band in the Raman measurement in BLG.[20,21] Clearly, a correct explanation of the experimental observations requires a detailed knowledge of the response of these phonon modes to the EEF from first principles. Such knowledge would also provide a necessary insight into the phonon and electron-phonon coupling and their effects on the transport performance of devices made of BLG.[23,24]

In this work, we present a first-principles study of the electric-field effects on the optical vibrations in BLG. The optical phonon modes with $q = 0$ are calculated using the density functional perturbation theory (DFPT)[25] as implemented in the QUANTUM ESPRESSO code[26] at the local density approximation (LDA) level. A norm-conserving pseudopotential[27] for carbon has been adopted to describe the core-valence interactions. The wave functions of the valence electrons are expanded in plane waves with a kinetic energy cutoff of 70 Ry. A vacuum region of 20 Å has been introduced to eliminate the artificial interaction between neighboring supercells along the z direction. The relaxed C-C bond length is 1.42 Å and the interlayer distance is 3.32 Å for the BLG. Details have been presented in our previous work.[28,29] To mimic the electric field, a sawtooth potential is applied to the bilayer graphene sheets perpendicularly. More realistic configurations, such as substrate-induced electric field,[30] should not change the physics significantly because of similar band gap opening. Dipole corrections have been considered throughout all calculations below.

Without EEF, BLG possesses a point group symmetry of D_{3d}. The two in-plane optical modes at $q = 0$ are low-branch E_g ($\omega = 1587$ cm^{-1}) and high-branch E_u ($\omega = 1592$ cm^{-1}) modes, as schematically shown in Figs. 1(b) and 1(a), respectively. Depicted in Figs. 2(b) and 2(a) are the two out-of-plane optical modes A_{1g} ($\omega = 891$ cm^{-1}) and A_{2u} ($\omega = 894$ cm^{-1}), respectively. We have calculated the phonon frequencies under various finite fields using DFPT. The variations of ω are within 2 cm^{-1} for electric fields up to 5 V/nm, indicating negligible field effects on the phonon frequency shift within the adiabatic approximation, in agreement with previous work.[32]

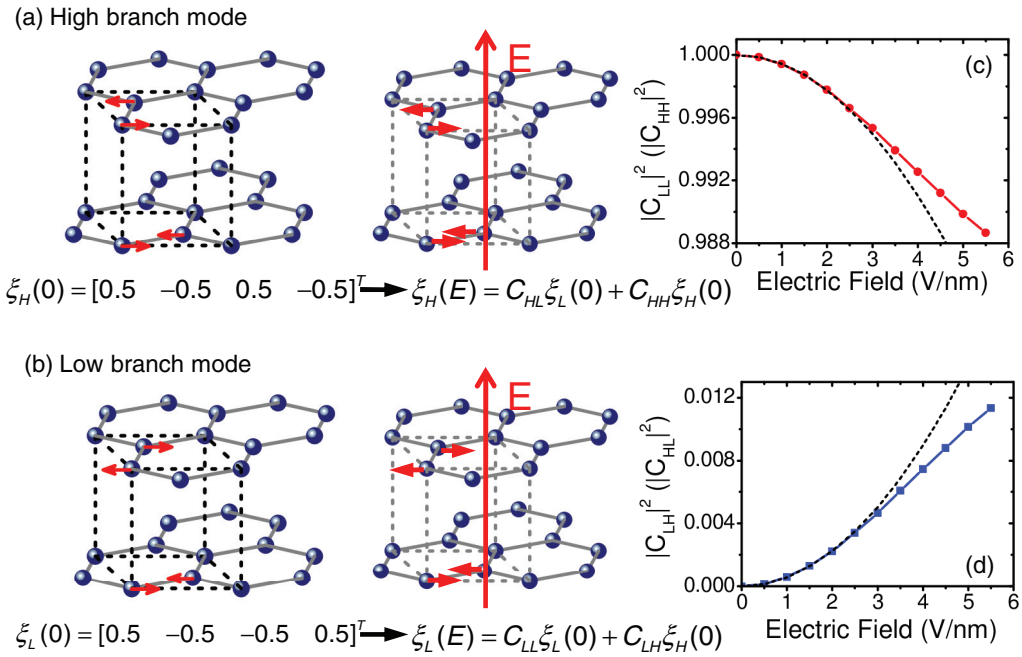

FIG. 1. (Color online) Schematic plots of the in-plane (a) high-branch mode with $\omega_H = 1592\ \mathrm{cm}^{-1}$ and (b) low-branch mode with $\omega_L = 1587\ \mathrm{cm}^{-1}$ under zero and finite electric fields, respectively. The calculated modes $\xi_L(E)$ and $\xi_H(E)$ under field can be decomposed using $\xi_L(0)$ and $\xi_H(0)$ as a complete basis set. The amplitude of (c) $|c_{LL}|^2$ ($|c_{HH}|^2$) and (d) $|c_{HL}|^2$ ($|c_{LH}|^2$) changes with respect to the field. The dashed lines are parabolic fitting of the data as $E < 2$ V/nm.

We then consider the phonon mode mixing induced by EEF. The applied EEF perpendicular to BLG will break the inversion symmetry of BLG, and the point group is reduced to C_{3v}. The two in-plane modes now belong to the E representation of C_{3v}, and both of them become Raman and IR active. Since

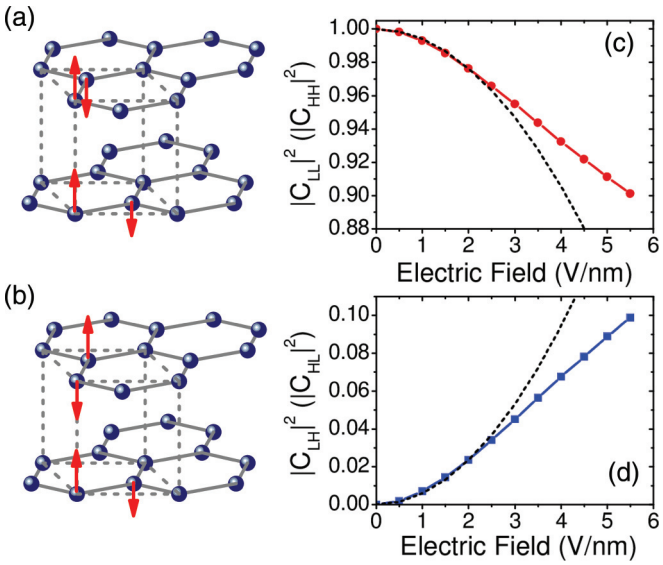

FIG. 2. (Color online) Schematic plots of the out-of-plane (a) high-branch A_{2u} mode with $\omega = 894\ \mathrm{cm}^{-1}$ and (b) low-branch A_{1g} mode with $\omega = 891\ \mathrm{cm}^{-1}$ under zero electric field. The calculated modes $\xi_L(E)$ and $\xi_H(E)$ under field can be decomposed using $\xi_L(0)$ and $\xi_H(0)$ as a complete basis set. The amplitude of (c) $|c_{LL}|^2$ ($|c_{HH}|^2$) and (d) $|c_{HL}|^2$ ($|c_{LH}|^2$) changes with respect to the field. The dashed lines are parabolic fitting of the data as $E < 2$ V/nm.

E is a two-dimensional representation, the two orthonormal eigenvectors of these modes form a complete set for the mixed in-plane modes. Because the frequencies of the E_g and E_u modes are close to each other, a finite electric field will be very likely to alter the phonon wave functions. Hereafter the (mixed) E_g and E_u modes are denoted as low-branch (L) and high-branch (H) modes, respectively, as shown in Fig. 1.

Quantitatively, the mixed amplitudes can be obtained by decomposition: $\xi_H(E) = c_{HL}\xi_L(0) + c_{HH}\xi_H(0)$ and $\xi_L(E) = c_{LL}\xi_L(0) + c_{LH}\xi_H(0)$, with $c_{\alpha\beta} = \xi_\alpha^\dagger(E)\xi_\beta(0)$ $(\alpha,\beta = L,H)$. The eigenvectors[34] $\xi_L(0) = [0.5, -0.5, -0.5, 0.5]^T$ and $\xi_H(0) = [0.5, -0.5, 0.5, -0.5]^T$ correspond to the E_g and E_u modes under zero electric field, respectively. The expansion coefficients satisfy $|c_{HL}|^2 + |c_{LL}|^2 = |c_{LH}|^2 + |c_{HH}|^2 = 1$, and $|c_{HL}|^2 = |c_{LH}|^2$. For a given electric field E, the amplitude of $|c_{LH}|^2$ ($|c_{HL}|^2$) shows the probability another mode contributes to the phonon wave function and is an indication of the mixing effect.

Figures 1(c) and 1(d) show the calculated $|c_{LL}|^2$ and $|c_{LH}|^2$ as a function of E, respectively. When $E < 2$ V/nm, the mixed component $|c_{LH}|^2$ increases parabolically and a polynomial fitting yields $|c_{LH}(E)|^2 = 5.6 \times 10^{-4}E^2$ with E in V/nm. When $E > 2$ V/nm, $|c_{LH}|^2$ increases linearly with respect to E. The slope is found to be 2.7×10^{-3}. Overall, the mixed component is within 1.2% with E up to 5 V/nm, implying a small mixing effect induced by EEF on the in-plane optical modes. In Ref. 15, Ando and Koshino analyzed the phonon Green's functions of in-plane modes in BLG and reported that these modes are strongly mixed by the asymmetrical potential difference arising from bottom gate doping and external electric field.[15] To clarify the effects of the charge doping and the external electric fields, we performed further calculations to

investigate the phonon eigenvectors for a charged BLG under an external electric field. Our results show that the phonon mode eigenvectors are still only slightly mixed (smaller than 1%) by the external electric field along with the charge doping.

Similar analyses can be applied to the out-of-plane modes, the low-branch A_{1g} and the high-branch A_{2u} modes. In Figs. 2(c) and 2(d), the amplitudes of the mixed components $|c_{LL}|^2$ and $|c_{LH}|^2$ are presented as a function of E, respectively. When $E < 2$ V/nm, the mixed component $|c_{LH}|^2$ increases parabolically as $|c_{LH}(E)|^2 = 5.9 \times 10^{-3} E^2$ with E in V/nm. When $E > 2$ V/nm, $|c_{LH}|^2$ increases linearly with a slope of 2.2×10^{-2}. From Figs. 2(c) and 2(d), EEF has dramatic effects on the mixing of the two out-of-plane modes; the mixing components reach 10% as $E = 5.5$ V/nm. This is nearly an order of magnitude larger than that for the in-plane modes. It was previously assumed that the electric field has negligible effects on the phonon eigenmodes.[16] In contrast, as demonstrated here, the out-of-plane phonon modes in layered systems could be significantly altered by EEF.

We then turn to the electron-phonon coupling (EPC) of the two in-plane modes. EPC plays a key role in understanding many phenomena,[6,7,9,10,14] especially the Raman frequency shift and broadening. The phonon self-energy $\Pi_{\mathbf{q}\nu}(\omega)$ of a phonon with wave vector $\mathbf{q}$, branch index ν, and frequency $\omega_{\mathbf{q}\nu}$ provides the renormalization and the damping of that phonon due to the interaction with other elementary excitations. Following the Migdal approximation, the self-energy induced by the EPC in BLG reads[14,31]

$$\Pi_{\mathbf{q}\nu}(\omega) = 2\sum_{mn}\int \frac{d\mathbf{k}}{\Omega_{\mathrm{BZ}}} \left|g^{\nu}_{mn}(\mathbf{k},\mathbf{q})\right|^2 \times \frac{[f(\epsilon_{n\mathbf{k}+\mathbf{q}}) - f(\epsilon_{m\mathbf{k}})][\epsilon_{n\mathbf{k}+\mathbf{q}} - \epsilon_{m\mathbf{k}}]}{(\epsilon_{n\mathbf{k}+\mathbf{q}} - \epsilon_{m\mathbf{k}})^2 - (\hbar\omega + i\eta)^2}, \quad (1)$$

where $\epsilon_{m\mathbf{k}}$ is the energy of an electronic state $|m\mathbf{k}\rangle$ with crystal momentum $\mathbf{k}$ and band index m, $f(\epsilon_{m\mathbf{k}})$ is the corresponding Fermi occupation, and η is a positive infinitesimal. A factor of 2 accounts for electron spin. For a given mode $\omega = \omega_0$, the phonon linewidth is $\gamma = -2\mathrm{Im}(\Pi_{\mathbf{q}\nu}(\omega_0))$ and the phonon frequency shift is $\Delta\omega = \frac{1}{\hbar}[\mathrm{Re}(\Pi_{\mathbf{q}\nu}(\omega_0)|_{E_F} - \Pi_{\mathbf{q}\nu}(\omega_0)|_{E_F=0})]$.

The EPC matrix elements in Eq. (1) are calculated using the frozen-phonon approach developed in our previous work.[29] We have considered the cases with and without the mixing effects and only a negligible difference has been noticed since the mixed amplitude is within 1.2% for the range of the electric fields considered. Below we only show the results with mixing effects included. Calculations of the phonon self-energy have been carried out on a dense 101×101 k grid within a minizone (0.2×0.2) enclosing the BZ corner $K(K')$ in the reciprocal space. This is equivalent to a 500×500 k-grid sampling in the whole Brillouin zone. By changing the Fermi level E_F in Eq. (1), the dependence of γ and $\Delta\omega$ on different doping levels can be investigated, assuming the EPC matrix elements are unchanged. This approximation is justified by the small dependence of the EPC matrix elements on doping for the Γ phonon modes in graphene.[33] For all the linewidths calculated below, a parameter of $\eta = 5$ meV has been used.

Figures 3(a) and 3(b) show the calculated linewidth γ for the low-branch (E_g) and high-branch (E_u) modes as a function of the Fermi level E_F and the electric-field strength

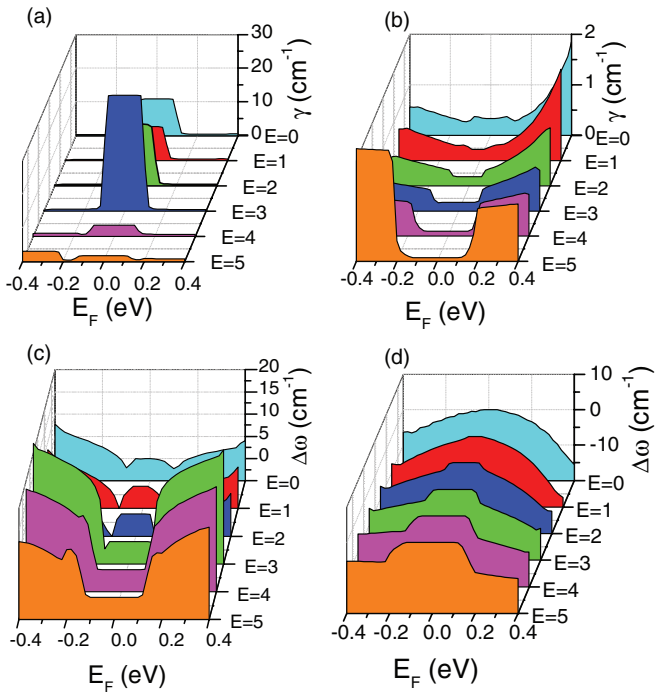

FIG. 3. (Color online) Calculated phonon linewidth γ of the (a) low-branch and (b) high-branch in-plane modes as a function of the Fermi level E_F as well as the electric field E (in V/nm). The corresponding frequency shifts $\Delta\omega$ are shown in (c) and (d), respectively. The neutrality point has been shifted to zero.

E, respectively. When the system is neutral ($E_F = 0$), the linewidth γ of the E_g mode increases from 9.0 cm^{-1} to 10 cm^{-1} as E increases from zero to 1 V/nm. It increases to the maximum of 30 cm^{-1} when $E = 3$ V/nm. After $E > 3$ V/nm, γ decreases to zero rapidly. As shown in Fig. 4(b), the largest γ at $E = 3$ V/nm is due to the fact that the electronic transition amplitude is the highest when the field-induced band gap $\sim$ 0.2 eV, close to the phonon energy. In contrast, when $E_F = 0$, the high-branch E_u mode exhibits nearly negligible linewidth for all the electric fields. This result clearly shows that only

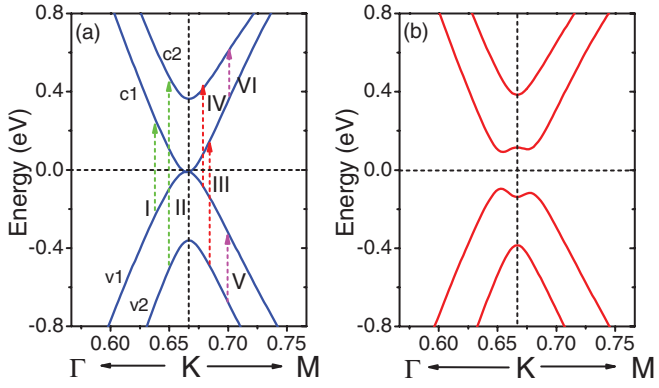

FIG. 4. (Color online) Band structure of BLG under (a) zero electric field and (b) electric field of $E = 3$ V/nm. As indicated in (a), the low-branch E_g mode couples with transitions I (v1-c1), II (v2-c2), while the high-branch E_u mode couples with transitions of III, IV, V, and VI. The neutrality point has been shifted to zero.

the low-branch E_g mode can possibly exhibit a large linewidth as observed in previous IR measurements[9] and thus resolves the discrepancy on the mode assignment.[9,10] The calculated phonon linewidth without field reproduces the features found in the previous DFT[35] and analytical calculations[14] and agrees reasonably well with the experimental data.[7] The evolution of γ for the E_g mode as a function of E also agrees quantitatively with that by Ando and Koshino.[15]

For a given field E, the linewidths of the two modes change dramatically with the doping level E_F. This can be understood from the selective coupling between the phonon modes and electronic bands. In the low-doping regime with $|E_F| < \hbar\omega_0/2 \sim 0.1$ eV, the low-branch mode can be in a resonant coupling with the electron-hole pair from the top valence band (v1) and the bottom conduction band (c1), as shown in Fig. 4. As a result, the linewidth of the low-branch mode is a constant within this doping range, as depicted in Fig. 3(a). Beyond this range, the linewidth of the E_g mode becomes nearly zero, while γ of the E_u mode increases. This is because the E_u mode couples with the two valence bands (v1 and v2) and conduction bands (c1 and c2), respectively, which has been discussed in detail in our previous work.[31] This feature is not captured by Ref. 15 because of their simplified band structure of BLG. In view of the slight mixing effect on the phonon mode, we conclude that it is mainly the band structure effect that plays a dominant role in the tunable interplay between electrons and phonons in BLG induced by EEF and E_F.

The corresponding frequency shifts $\Delta\omega$ are presented in Figs. 3(c) and 3(d), respectively. In particular, the low-branch E_g mode exhibits a frequency increase (hardening) when the $|E_F| > \hbar\omega_0/2$. In contrast, the high-branch E_u mode softens with the increase of $|E_F|$. As a result, two distinguishable peaks will appear in the Raman or IR spectra of gated BLG. Since the frequency of the E_u mode (1592 cm^{-1}) is higher than the E_g mode (1587 cm^{-1}), one expects a crossing of the two branches as $|E_F|$ increases. This is in agreement with the Raman data by Yan *et al.*[20] From Figs. 3(c) and 3(d), for a higher E, the E_g mode can be tuned by $|E_F|$ and hardens even faster, implying an interesting interplay between EEF, electrons, and phonons in BLG.

In summary, we found that the electric field only slightly mixes the two in-plane modes, while inducing a relatively large change on the out-of-plane modes. Because of the broken symmetry, the two in-plane modes become Raman and IR active, and are detectable by both Raman and IR spectroscopy. The delicate electron-phonon coupling can be tuned through doping and an external gate field. It is mainly the band structure of BLG, tunable by external field and charge carrier densities, that dominates the dependence of the phonon linewidth and frequency shift as a function of E_F and E. Our findings have revealed the external field effects on the phonon frequency renormalization observed in experiment, and may also be useful to study the field effects on other layered systems such as multilayer graphene.

J.A.Y. thanks Mei-Yin Chou and Kalman Varga for fruitful discussions. This work used the computer resources of Carver at NERSC and Kraken at the National Institute for Computational Sciences under an XSEDE startup allocation (Request No. DMR110111).

*jiaanyan@gmail.com

[1] J. B. Oostinga, Hubert B. Heersche, Xinglan Liu, Alberto F. Morpurgo, and Lieven M. K. Vandersypen, Nat. Mater. **7**, 151 (2007).

[2] Yuanbo Zhang, Tsung-Ta Tang, Caglar Girit, Zhao Hao, Michael C. Martin, Alex Zettl, Michael F. Crommie, Y. Ron Shen, and Feng Wang, Nature (London) **459**, 820 (2009).

[3] T. Ohta, A. Bostwick, T. Seyller, K. Horn, and E. Rotenberg, Science **313**, 951 (2006).

[4] D. K. Efetov, P. Maher, S. Glinskis, and P. Kim, Phys. Rev. B **84**, 161412(R) (2011).

[5] T. Taychatanapat and P. Jarillo-Herrero, Phys. Rev. Lett. **105**, 166601 (2010).

[6] L. M. Malard, D. C. Elias, E. S. Alves, and M. A. Pimenta, Phys. Rev. Lett. **101**, 257401 (2008).

[7] J. Yan, E. A. Henriksen, P. Kim, and A. Pinczuk, Phys. Rev. Lett. **101**, 136804 (2008).

[8] A. Das, B. Chakraborty, S. Piscanec, S. Pisana, A. K. Sood, and A. C. Ferrari, Phys. Rev. B **79**, 155417 (2009).

[9] A. B. Kuzmenko, L. Benfatto, E. Cappelluti, I. Crassee, D. van der Marel, P. Blake, K. S. Novoselov, and A. K. Geim, Phys. Rev. Lett. **103**, 116804 (2009).

[10] T.-T. Tang, Y. Zhang, C.-H. Park, B. Geng, C. Girit, Z. Hao, M. C. Martin, A. Zettl, M. F. Crommie, S. G. Louie, Y. R. Shen, and F. Wang, Nat. Nanotechnol. **5**, 32 (2010).

[11] J. Yan, M.-H. Kim, J. A. Elle, A. B. Sushkov, G. S. Jenkins, H. M. Milchberg, M. S. Fuhrer, and H. D. Drew, arXiv:1111.1202.

[12] Z. Q. Li, E. A. Henriksen, Z. Jiang, Z. Hao, M. C. Martin, P. Kim, H. L. Stormer, and D. N. Basov, Phys. Rev. Lett. **102**, 037403 (2009).

[13] K. F. Mak, C. H. Lui, J. Shan, and T. F. Heinz, Phys. Rev. Lett. **102**, 256405 (2009).

[14] T. Ando, J. Phys. Soc. Jpn. **76**, 104711 (2007).

[15] T. Ando and M. Koshino, J. Phys. Soc. Jpn. **78**, 034709 (2009).

[16] J. M. Worlock and P. A. Fleury, Phys. Rev. Lett. **19**, 1176 (1967).

[17] A. F. W. Klukhuhn, J. Bruining, B. Klootwijk, and J. van der Elsken, Phys. Rev. Lett. **25**, 380 (1970).

[18] L. Brillson and E. Burstein, Phys. Rev. Lett. **27**, 808 (1971).

[19] S. Berweger, C. C. Neacsu, Y. Mao, H. Zhou, S. S. Wong, and M. B. Raschke, Nat. Nanotechnol. **4**, 496 (2009).

[20] J. Yan, T. Villarson, E. A. Henriksen, P. Kim, and A. Pinczuk, Phys. Rev. B **80**, 241417(R) (2009).

[21] P. Gava, M. Lazzeri, A. M. Saitta, and F. Mauri, Phys. Rev. B **80**, 155422 (2009).

[22] M. Bruna and S. Borini, Phys. Rev. B **81**, 125421 (2010).

[23] Zhen Yao, Charles L. Kane, and Cees Dekker, Phys. Rev. Lett. **84**, 2941 (2000).

[24] P. Lichtenberger, O. Morandi, and F. Schürrer, Phys. Rev. B **84**, 045406 (2011).

[25]S. Baroni, S. de Gironcoli, and A. Dal Corso, Rev. Mod. Phys. **73**, 515 (2001).
[26]P. Giannozzi *et al.*, J. Phys. Condens. Matter **21**, 395502 (2009).
[27]N. Troullier and J. L. Martins, Phys. Rev. B **43**, 1993 (1991).
[28]J. A. Yan, W. Y. Ruan, and M. Y. Chou, Phys. Rev. B **77**, 125401 (2008).
[29]J. A. Yan, W. Y. Ruan, and M. Y. Chou, Phys. Rev. B **79**, 115443 (2009).
[30]D. Ziegler, P. Gava, J. Güttinger, F. Molitor, L. Wirtz, M. Lazzeri, A. M. Saitta, A. Stemmer, F. Mauri, and C. Stampfer, Phys. Rev. B **83**, 235434 (2011).
[31]J. A. Yan, K. Varga, and M. Y. Chou, Phys. Rev. B **86**, 035409 (2012).
[32]S. Pisana, M. Lazzeri, C. Casiraghi, K. S. Novoselov, A. K. Geim, A. C. Ferrari, and F. Mauri, Nat. Mater. **6**, 198 (2007).
[33]C. Attaccalite, L. Wirtz, M. Lazzeri, F. Mauri, and A. Rubio, Nano Lett. **10**, 1172 (2010).
[34]The phonon eigenvectors consist of three components (x, y, z) for each of the four atoms in the unit cell of BLG (as indicated in Figs. 1 and 2). For the doubly degenerate in-plane modes, we only consider the nonzero x vibrations. All the y and z components are suppressed since they are zero. Similarly, we suppress the x and y components for the out-of-plane modes below.
[35]C.-H. Park, F. Giustino, M. L. Cohen, and S. G. Louie, Phys. Rev. Lett. **99**, 086804 (2007); Nano Lett. **8**, 4229 (2008).